

Saturation-recovery metabolic imaging of hyperpolarised ¹³C pyruvate

R. F. Schulte¹, M. I. Menzel¹, E. Weidl², M. Janich^{1,3}, M. Schwaiger², and F. Wiesinger¹

¹GE Global Research, Munich, Germany, ²Nuclear Medicine, Technische Universität München, Munich, Germany, ³Chemistry, Technische Universität München, Munich, Germany

Introduction

Metabolic imaging with hyperpolarised [¹³C]pyruvate (Pyr) enables the real-time detection of metabolism [1]. The resulting encoding challenge for MR is five-dimensional: three spatial, one spectral and ideally one temporal dimension in order to extract dynamic information. Furthermore, the polarisation decays non-recoverably with $T_1 \approx 30$ s (in vivo). One approach to address this challenge is to use spectral-spatial (SPSP) excitation [2,3]. In [2], SPSP pulses are used to excite the whole spectrum with different weights. However, an EPSI (echo-planar spectroscopic imaging) readout is still required to encode spectral and spatial dimensions. In [3], it is used to dynamically image lactate with a small tip angle and EPI readout. In this work, SPSP pulses are used to image multiple metabolites at different flip angles by selectively exciting single resonances and imaging them with a single-shot spiral readout. This is combined with a saturation-recovery experiment to directly detect the build-up of lactate (Lac) and alanine (Ala).

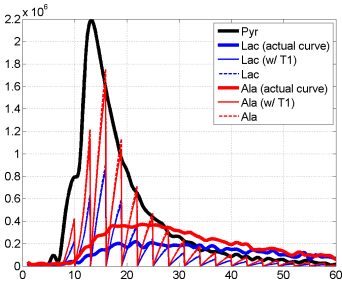


Fig. 1: Simulated signal response for saturation recovery based on measured metabolic time curves (assuming $k_{P \rightarrow A} = 0.014$, $k_{P \rightarrow L} = 0.027$ and flip angles of 90° (Lac, Ala) and 5° (Pyr)). The signal level is high despite the short build-up time (here 3 s) and T_1 can be neglected.

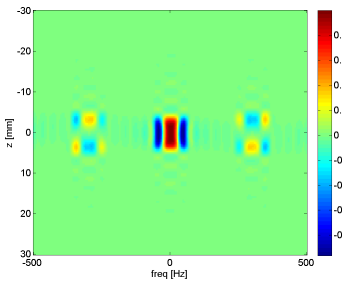


Fig. 2: Bloch simulation of the SPSP excitation profile (real-part only). It is composed of 15 sub-lobes. The side-band artefact region is chosen not to coincide with any metabolites.

Theory and Methods

Pyruvate is enzymatically converted in cells into lactate and alanine. Mathematically, this conversion can be described by a simplified model $dM_X/dt = k_{P \rightarrow X} M_P - 1/T_{1,X,eff} M_X$, where M denotes the detectable magnetisation of Pyr (P) or Lac/Ala (X), $k_{P \rightarrow X}$ / $k_{P \rightarrow X}$ the metabolic conversion rate constants and $T_{1,X,eff}$ the effective decay time including T_1 , excitation and back conversion. Although normally depletion dominates build-up (i.e. $T_{1,eff} < 1/k_{P \rightarrow X}$), relaxation can still be neglected for short build-up times (T_{bup}). Hence, after crushing all existing metabolite polarisation M_X and waiting a suitable time T_{bup} , one will get predominantly signal governed by $k_{P \rightarrow X} = S_X \sin \alpha_P / (T_{bup} S_P \sin \alpha_X)$, where S denotes the detected signal and α the flip angle. The validity of this assumption was verified by simulations with typical $k_{P \rightarrow X}$ and $T_{1,eff}$ values (Fig. 1).

Spectral-spatial (SPSP) pulses were designed with pass- and stop-band frequencies of 30 and 150 Hz, respectively (Fig. 2), 15 sub-lobes, a total duration of 26 ms and a partly self-refocused phase to minimise the remaining linear phase in the spectral domain. The sidebands were chosen to appear at 300 Hz (artefact) and 600 Hz (aliasing) in order to minimise mutual contamination of Pyr, Lac and Ala signal. The SPSP pulse was shifted during different excitations to the resonance frequencies of Pyr (-392 Hz), Lac (0 Hz) and Ala (-215 Hz), which were excited with 5° , 90° and 90° , respectively. Lac and Ala were excited twice in order to increase crushing efficiency, with only the first excitation being used for image reconstruction. With $TR = 0.5$ s and an overall excitation scheme of (Pyr – Lac – Lac – Pyr – Ala – Ala – Pyr – dummy), the overall TR for a single time point was 4s and $T_{bup} = 3.5$ s.

The SPSP pulse was implemented on a GE Signa Excite scanner (GE Healthcare, Milwaukee, USA) in a pulse-and-acquire sequence with single-shot spiral readout (FOV=8cm, nominal resolution 38x38, $G_{max} = 23$ mT/m, $S_{max} = 77$ T/m/s). 2.5ml/kg of 80mM hyperpolarised [¹³C]Pyr solution was injected into the tail vein of a male Buffalo rat with a subcutaneous hepato-cellular carcinoma (approved by governmental ethics commission). Acquisition was started prior to injection, with the sequence being repeated for about 1 minute.

Results and Discussion

The proposed acquisition scheme efficiently separates the encoding into spectral-spatial excitation and 2D spatial in-plane encoding, hence considerably accelerating image encoding and simplifying image reconstruction. Using 90° excitation for Lac/Ala results in effective signal levels comparable to continuous small flip angle excitation, yet with the advantage of simplified biological interpretation. Regions with high Lac or Ala signal are not necessarily regions with high metabolic activity, as seen in Fig 3 in the lower part of the abdomen. Hence, an effective metabolic rate image $k_{P \rightarrow X}$ is a more direct and physiological contrast. The effective metabolic rate is strongly increased for Ala in the tumour, while Lac shows elevation in both tumour and muscles.

Spectral contamination from high pyruvate peak is only visible for the first point when the bolus reaches the vasculature, but has not been converted yet. Pyr signal was still strong in the vessels during the 3rd time point, leading to underestimated rates of $k_{P \rightarrow L}$ and $k_{P \rightarrow A}$ (dark circular region around vessel in 3). The obtained effective rate constants slightly increase over time, indicating inflowing signal of lactate and alanine or non-linear kinetics. Inflow effects can be further minimised by saturating Lac/Ala over the whole object. In summary, saturation recovery metabolic imaging describes a novel method for the direct assessment of spatially-resolved metabolic rate constants.

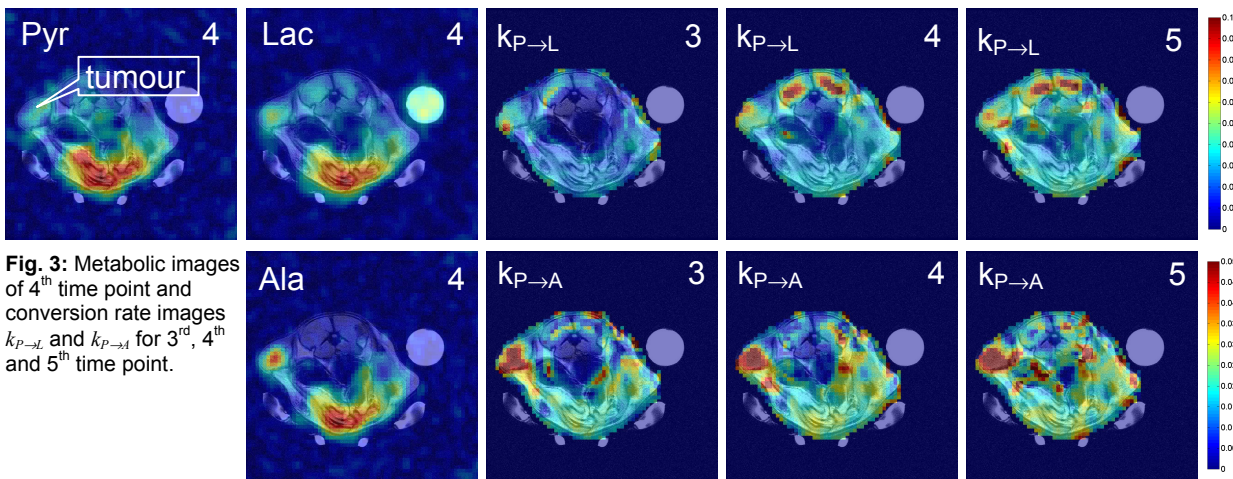


Fig. 3: Metabolic images of 4th time point and conversion rate images $k_{P \rightarrow L}$ and $k_{P \rightarrow A}$ for 3rd, 4th and 5th time point.

References

- [1] Golman, PNAS 2003, 100, 10435.
- [2] Larson, JMR 2008, 191, 121.
- [3] Cunningham, JMR 2008, 193, 139.

Acknowledgements

This work was partly funded by BMBF MobiTUM grant # 01EZ0827.